

# Interphase force analysis for air-water bubbly flow in a multiphase rotodynamic pump

Zhiyi Yu

*School of Mechanical Engineering, Beijing Institute of Technology, Beijing,  
China, and*

Baoshan Zhu and Shuliang Cao

*State Key Laboratory of Hydrosience and Engineering,  
Department of Thermal Engineering, Tsinghua University,  
Beijing, China*

## Abstract

**Purpose** – Interphase forces between the gas and liquid phases determine many phenomena in bubbly flow. For the interphase forces in a multiphase rotodynamic pump, the magnitude analysis was carried out within the framework of two-fluid model. The purpose of this paper is to clarify the relative importance of various interphase forces on the mixed transport process, and the findings herein will be a base for the future study on the mechanism of the gas blockage phenomenon, which is the most challenging issue for such pumps.

**Design/methodology/approach** – Four types of interphase forces, i.e. drag force, lift force, virtual mass force and turbulent dispersion force (TDF) were taken into account. By comparing with the experiment in the respect of the head performance, the effectiveness of the numerical model was validated. In conditions of different inlet gas void fractions, bubble diameters and rotational speeds, the magnitude analyses were made for the interphase forces.

**Findings** – The results demonstrate that the TDF can be neglected in the running of the multiphase rotodynamic pump; the drag force is dominant in the impeller region and the outlet extended region. The sensitivity analyses of the bubble diameter and the rotational speed were also performed. It is found that larger bubble size is accompanied by smaller predicted drag but larger predicted lift and virtual mass, while the increase of the rotational speed can raise all the interphase forces mentioned above.

**Originality/value** – This paper has revealed the magnitude information and the relative importance of the interphase forces in a multiphase rotodynamic pump.

**Keywords** Sensitivity analysis, Bubbly flow, Interphase force, Magnitude analysis, Multiphase rotodynamic pump, Two-fluid model

**Paper type** Research paper



**Nomenclature**

$IGVF$	inlet gas void fraction, dimensionless	$\alpha_{VM}$	virtual mass acceleration, $m/s^2$
$VMF$	virtual mass force, N	$I$	axial direction, dimensionless
$TDF$	turbulent dispersion force, N	$J$	circumferential direction, dimensionless
$w$	velocity, m/s	$K$	radial direction, dimensionless
$p$	pressure, Pa	$u_2$	circumferential velocity at the tip of impeller in the outlet, m/s
$M$	total interphase force per unit volume, $N/m^3$	$v_{m2}$	mean meridional velocity at the outlet, m/s
$f$	mass force relevant to the rotation of the impeller, $m/s^2$	$H$	pump head, m
$a_1$	constant in SST- $k-\omega$ model, dimensionless	$x$	mass flow rate ratio of gas to the two-phase mixture
$k$	turbulent kinetic energy, $m^2/s^2$	$g$	gravitational constant, $m/s^2$
$S$	invariant measure of the strain rate	$n$	rotational speed, rpm
$F_2$	blending function in SST- $k-\omega$ model	$z$	axial coordinate, m
$M^D$	drag force per unit volume, $N/m^3$	$L$	axial length of the computational domain, m
$M^L$	lift force per unit volume, $N/m^3$		
$M^{VM}$	virtual mass force per unit volume, $N/m^3$		
$M^{TD}$	turbulent dispersion force per unit volume, $N/m^3$	<i>Greek symbols</i>	
$C_D$	drag coefficient, dimensionless	$\alpha$	void fraction, dimensionless
$C_{D1}$	drag coefficient for the viscous regime, dimensionless	$\rho$	density of phase k, $kg/m^3$
$C_{D2}$	drag coefficient for the distorted regime, dimensionless	$\tau$	viscous stress tensor, Pa
$C_L$	lift coefficient, dimensionless	$\mu$	molecular viscosity, Pa.s
$C_{TD}$	coefficient of the turbulent dispersion, dimensionless	$\mu_t$	turbulent viscosity, Pa.s
$D_b$	bubble diameter, m	$\omega$	turbulent eddy frequency, 1/s
$w_R$	relative velocity between the two phases, m/s	$\sigma$	surface tension coefficient, N/m
$Re_b$	bubble Reynolds number, dimensionless	$\psi$	head coefficient, dimensionless
$C_{VM}$	virtual mass coefficient, dimensionless	$\varphi$	flow rate coefficient, dimensionless
		<i>Subscripts</i>	
		k	phase
		gas	gas phase
		liq	liquid phase
		mix	mixture
		tp	two-phase

**1. Introduction**

As one of the two leading types of multiphase pumping equipment, rotodynamic pumps has received now a widespread acceptance because it can provide a large flow rate and it is applicable to multiphase flow containing small sand particles (Cao *et al.*, 2005). The big challenge of this technology is to overcome the phenomena of gas blockage and systematical instability under the conditions of high gas void fraction. To solve this problem, people need to know the gas-liquid separation process by experimental or numerical techniques, so as to improve the hydraulic design of the pump impeller. However, due to the financial and technical limitation, experimental investigations can now be used only for the flow in non-rotating parts or some special

working conditions (Hajem *et al.*, 2001; Tan *et al.*, 2012, 2014), and thus computational fluid dynamics (CFD) has become the only applicable means for the moment.

The two-fluid model is one of the basic two-phase models developed for simulating the small-length-scale bubbles, such as in bubbly or dispersed flow (Yan and Che, 2010). Through this model, interphase momentum transfer between the two phases can be taken into account. To predict the flow pattern inside the bubble column, the Eulerian-Eulerian approach often uses the drag force as the predominant interphase force (Pourtousi *et al.*, 2014). Many studies have used only the drag force in order to predict hydrodynamic properties in bubbly flow (Gupta and Roy, 2013; Zhang *et al.*, 2006; Laborde-Boutet *et al.*, 2009; Chen *et al.*, 2005). In the meanwhile, some studies have used other interphase forces in the solving of the momentum equation. For example, Zhang *et al.* (2006), Deen (2001), Diaz *et al.* (2008) considered drag, lift and virtual mass forces (VMF) for their simulations; Tabib *et al.* (2008) and Deen (2001) incorporated drag, lift and turbulent dispersion forces (TDFs) into their investigations, while Bai *et al.* (2011) included drag, lift, added mass and wall lubrication forces.

Generally, a more inclusive interphase closure model will result in more accurate simulation. In some cases, however, the effects of some interphase forces can be neglected to save the computational cost and time (Zhang *et al.*, 2006; Tabib *et al.*, 2008; Deen *et al.*, 2001; Krepper *et al.*, 2009; Dhotre *et al.*, 2013). For instance, the study of Tabib *et al.* (2008) shown that there is no significant contribution of VMF on the simulation of local hydrodynamics of bubble column. This may be attributed to the fact that the effect of the acceleration and deceleration of the liquid is restricted to small end regions of the column. Similarly, for the gas-liquid two-phase flow in a rotodynamic pump, the interphase forces may be of unequal importance, which is depending on the flowrate, rotational speed, gas void fraction and pump structure. Therefore, magnitude analysis is needed to simplify the interphase closure model. In addition, such analysis will help us to understand the mechanism of gas-liquid separation.

In this paper, the magnitude analysis is presented for the interphase forces in a multiphase rotodynamic pump within the framework of two-fluid model. Our focus is on the magnitude variation of the drag force and non-drag forces in different working conditions. The paper is organized as follows. First, the adopted numerical strategy including the governing equations, the interphase closure model as well as the mesh and boundary conditions are presented. Then, a validation of the numerical model is carried out according to the experimental data of the head performance. Before conclusions, the magnitude variations of the interphase forces in different working conditions are discussed.

## 2. Mathematical modeling

### 2.1 Two-fluid formulation

In recent decades, significant developments in the two-phase flow formulation have been accomplished by introducing and improving the two-fluid model. The two-fluid model can be considered the most detailed and accurate macroscopic formulation of the thermofluid dynamics of two-phase flow (Levy *et al.*, 2006; Yang and Zhang, 2005; Seixlack and Barbazelli, 2009; Benhmidene *et al.*, 2011). This model treats the general case by modeling each phase or component as a separate fluid with its own set of governing balance equations.

In the present work, the two-fluid model is used to predict the bubbly flow in a multiphase rotodynamic pump impeller. As our objective is to obtain the fundamental

magnitude information of the interphase forces, the simulations are carried out in a steady mode. Here, water and air are taken as the continuous phase and dispersed phase, respectively. When assuming the flow to be isothermal and ignoring interphase mass transfer, the energy equations can be skipped and no source or diffusion terms appear in the mass balances. The conservation equations for incompressible turbulent flow can be written as follows.

Continuity equation:

$$\nabla \cdot (\alpha_k \rho_k \mathbf{w}_k) = 0 \quad (1)$$

Momentum transfer equations:

$$\nabla \cdot (\alpha_k \rho_k \mathbf{w}_k \mathbf{w}_k - \alpha_k \boldsymbol{\tau}) = -\alpha_k \nabla p + \mathbf{M}_k + \alpha_k \rho_k \mathbf{f}_k \quad (2)$$

where the subscript  $k$  is the phase indicator with  $k = \text{liquid}$  for liquid phase and  $k = \text{gas}$  for gas phase.  $\alpha_k$ ,  $\rho_k$  and  $w_k$  denote the void fraction, the density and the velocity, respectively. The pressure  $p$  is shared by both fluids.  $M_k$  is the total interphase force acting on phase  $k$ ,  $f_k$  is the mass force relevant to the rotation of the impeller, which includes the centrifugal force and the Coriolis force.  $\tau$  denotes the viscous stress tensor concerning molecular viscosity as well as turbulence viscosity.

The turbulent eddy viscosity is formulated based on the SST- $k-\omega$  model. This model uses Wilcox model, i.e. the original  $k-\omega$  model at the walls, and  $k-\varepsilon$  model away from walls and solves the problem with the free stream turbulence in the latter part. The use of a  $k-\omega$  formulation in the inner parts of the boundary layer makes the model directly usable all the way down to the wall through the viscous sublayer. When the SST- $k-\omega$  switches to the  $k-\varepsilon$  model in the free stream, it avoids the common  $k-\omega$  problem that the model is too sensitive to the inlet free stream turbulence properties (Menter, 1994). Moreover, a blending factor ensures a smooth transition between the two models. It is generally believed that the SST- $k-\omega$  results in relatively good solutions for the flow with a large area of separation. Under this model, the turbulent viscosity is computed as follows:

$$\mu_t = \frac{\rho_{\text{mix}} a_1 k}{\max(a_1 \omega, S F_2)} \quad (3)$$

where the mixed density is calculated by  $\rho_{\text{mix}} = \alpha_{\text{liq}} \rho_{\text{liq}} + \alpha_{\text{gas}} \rho_{\text{gas}}$ ;  $a_1$  is a model constant and  $a_1 = 5/9$ ;  $S$  is an invariant measure of the strain rate and  $F_2$  is a blending function in this turbulence model.

## 2.2 Interphase forces

The interphase forces, denoted by  $M_k$ , is a sum of forces associated with drag, lift, virtual mass, turbulent dispersion as well as the Basset effect and the Magnus effect. The Basset term, depending on the acceleration history up to the present time, is important only in the initial phase of the acceleration (Liu, 1993). As the focus of this study is on the interphase forces in the normal running phase of the pump, the Basset effect is neglected. The Magnus effect is caused by a pressure differential between both sides of the particle resulting from the velocity differential due to rotation. When the particle size is small or the spin velocity is low, the Magnus force is negligibly small compared to the drag force (Johnson, 1998). For the present study, the Magnus force is

not considered as the rotation of the gas bubbles is assumed negligible. Therefore, the total interphase force acting between the two phases can be expressed as follows:

$$\mathbf{M}_k = \mathbf{M}_k^D + \mathbf{M}_k^L + \mathbf{M}_k^{VM} + \mathbf{M}_k^{TD} \quad (4)$$

where the individual terms on the right hand side are, respectively, the drag force, lift force, VMF and TDF. The drag force per unit volume for spherical gas bubbles is given by:

$$\mathbf{M}_{liq}^D = -\mathbf{M}_{gas}^D = \frac{3}{4}C_D \frac{\rho_{liq}}{D_b} \alpha_{gas} |\mathbf{w}_R| \mathbf{w}_R \quad (5)$$

where  $\mathbf{w}_R$  is the relative velocity between the two phases;  $D_b$  is the diameter of gas bubbles and  $C_D$  is the drag coefficient given by Tabib and Schwarz (2011):

$$C_D = \max(C_{D1}, C_{D2}) \quad (6)$$

where  $C_{D1}$  and  $C_{D2}$  are the drag coefficient for the viscous regime and the distorted regime, respectively, and are expressed as follows:

$$C_{D1} = \frac{24}{Re_b} (1 + 0.1 Re_b^{0.75}) \quad (7)$$

$$C_{D2} = \frac{2}{3} D_b \sqrt{\frac{(\rho_{liq} - \rho_{gas})g}{\sigma}} (1 - \alpha_{gas})^{-0.5} \quad (8)$$

The lift force, which arises from a velocity gradient of the continuous phase in the lateral direction, can be described as:

$$\mathbf{M}_{liq}^L = -\mathbf{M}_{gas}^L = C_L \alpha_{gas} \rho_{liq} (\mathbf{w}_{gas} - \mathbf{w}_{liq}) \times (\nabla \times \mathbf{w}_{liq}) \quad (9)$$

here, the lift coefficient  $C_L$  equals 0.5, which is the most common value for bubbly flow (Mohajerani *et al.*, 2012).

The third term in Equation (4) represents the VMF that comes into play when one phase is accelerating relative to the other one. In the case of gas-liquid two-phase flow, this force can be described by the following expression (Kendoush, 2005):

$$\mathbf{M}_{liq}^{VM} = -\mathbf{M}_{gas}^{VM} = \rho_{liq} C_{VM} \alpha_{gas} \mathbf{a}_{VM} \quad (10)$$

here, the value of  $C_{VM} = 0.5$  has been often used for spherical bubbles (Pourtousi *et al.*, 2014);  $\mathbf{a}_{VM}$  is the virtual mass acceleration vector written as:

$$\mathbf{a}_{VM} = (\mathbf{w}_{gas} \cdot \nabla) \mathbf{w}_{gas} - (\mathbf{w}_{liq} \cdot \nabla) \mathbf{w}_{liq} \quad (11)$$

The final term in Equation (4) is the TDF, which signifies the turbulent diffusion of the dispersed phase by the eddies in the continuous phase. The turbulent dispersion model is inspired by the analogy with the thermal diffusion of the air molecules in the atmosphere (Tabib *et al.*, 2008):

$$\mathbf{M}_{liq}^{TD} = -\mathbf{M}_{gas}^{TD} = -C_{TD} \rho_{liq} k \nabla \alpha_{liq} \quad (12)$$

where  $C_{TD}$  is the coefficient of the turbulent dispersion, equals to 0.1 as suggested by Lahey *et al.* (1993) and Bertodano *et al.* (1994). Troshko and Hassan (2001) believed that this value was selected based on the similarity of the coefficient and the eddy diffusivity constant.

### 2.3 Computational mesh and strategies

To avoid the gas-liquid separation more effectively, the wrap angle of the impeller blade is designed to be much larger (approximately  $220^\circ$  for this pump), and the passage is much narrower in the radial direction than the usual ones. However, such design also makes the generation of high quality mesh much more difficult. To solve this problem, the hybrid mesh generated by the software ICEM\_CFD 12.1 is used, i.e. the structured mesh is adopted for the inlet and outlet extended region, while the unstructured mesh for the impeller region, as shown in Figure 1, where  $I, J, K$  are defined as the axial direction, the circumferential direction and the radial direction, respectively..

In the calculation, the commercial CFD software ANSYS\_CFX 12.1 is used, coupled with the CFX expression language to implement the models of the four interphase forces as well as the pump head under two-phase condition, which will be described in the next section. The boundary conditions are set as follows: at the inlet, the axial velocity is specified according to the flow rate, and at the outlet, an averaged static pressure is given; at the wall boundaries (the pressure and suction surfaces, the hub and shroud walls), the non-slip condition of viscous fluid is used for both phases; for the three pairs of circumferential boundaries, the rotational periodic condition is imposed.

### 3. Validation of the numerical model

To assure the reliability of the interphase force analysis, the head performances are compared between the simulation and the experiment (Cao *et al.*, 2005). Taking into account the mass flow rate ratio of gas to the mixture, denoted by  $x$ , the head of the pump operating under gas-liquid two-phase flow condition can be obtained by:

$$H_{tp} = (1-x)H_{liq} + xH_{gas} \quad (13)$$

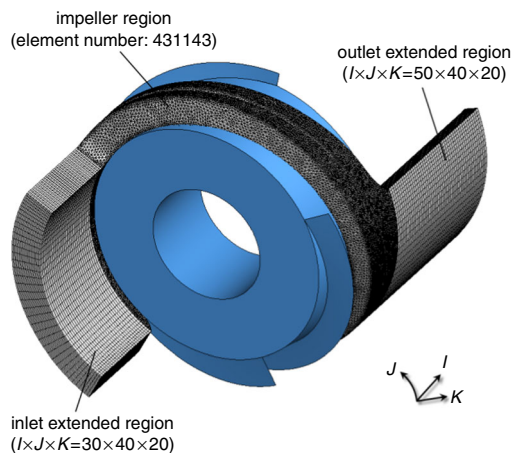


**Figure 1.**  
Impeller geometry  
and the hybrid mesh  
for flow analysis

where  $H_{liq}$  and  $H_{gas}$  are the heads for the liquid phase and gas phase, respectively, and they are calculated through the flow rate weighted averaged method (Yu, 2005). Then, a head coefficient  $\psi$  is defined as follows:

$$\psi = gH_{tp}/u_2^2 \tag{14}$$

here,  $u_2$  denotes the circumferential velocity at the tip of impeller in the outlet.

Similarly, concerning the through flow property, a total volume flow rate coefficient  $\varphi$  is defined as follows:

$$\varphi = v_{m2}/u_2 \tag{15}$$

where  $v_{m2}$  denotes the mean meridional velocity at the outlet of the pump impeller. The coefficient  $\varphi$  may be divided into two components, i.e.  $\varphi = \varphi_{gas} + \varphi_{liq}$ , where  $\varphi_{gas}$  and  $\varphi_{liq}$  denote the gas and the liquid flow rate coefficient, respectively. Then, the inlet gas void fraction (*IGVF*) can be calculated by  $IGVF = \varphi_{gas}/\varphi$ .

According to the experimental data, the optimum working condition when the rotational speed  $n$  equals 1500 rpm is that  $\varphi_{liq} = 0.081$  and  $\varphi = 0.095$ ; when  $\varphi_{liq} = 0.081$ , the head coefficient  $\psi$  is found to decrease nearly linearly with the increase of gas volume flow rate (Cao *et al.*, 2005). Here, this series of working conditions, listed in Table I, is selected for the validation of the numerical model.

Another important issue on the numerical model is the setting of the bubble size. According to the observation with a high speed camera for the optimum working condition, the bubble size near the outlet of the diffuser is mostly 0.4-1.0 mm when *IGVF* is 10 percent (Falcimaigne *et al.*, 2002). Due to the lack of other statistical data, the bubble diameter  $D_b$  in this study is set 0.4, 0.7 and 1.0 mm, respectively.

Figure 2 illustrates the head performance of the multiphase pump from the experiment and the simulation where different bubble diameters are used. For smaller values of  $\varphi$  (the former four cases in Table I), the numerical predictions with  $D_b = 0.4$  mm agree well with the experiment; with the increase of  $\varphi$  (higher *IGVF*), larger bubble diameter is inclined to behave better. This is reasonable because the bubbles tend to coalesce in higher *IGVF* condition and become larger. For the latter two cases with *IGVF* = 35.2 percent and *IGVF* = 40.0 percent, the errors are large. Therefore, the bubble size should be set more accurately based on future experimental study. Moreover, the regime transition in the flow passage in high *IGVF* conditions may probably be a key factor affecting the precision, because the models of interphase forces listed in section 2.2 need to be corrected for non-bubbly flow. In the following analyses, we are focussed on the former five cases listed in Table I for reliability.

**Table I.**  
Working conditions  
in the experiment

No.	1	2	3	4	5	6	7
$\varphi$	0.090	0.095	0.101	0.108	0.116	0.125	0.135
<i>IGVF</i> (%)	10.0	14.7	19.8	25.0	30.2	35.2	40.0
<b>Notes:</b> $\varphi_{liq} = 0.081$ ; $n = 1,500$ rpm							

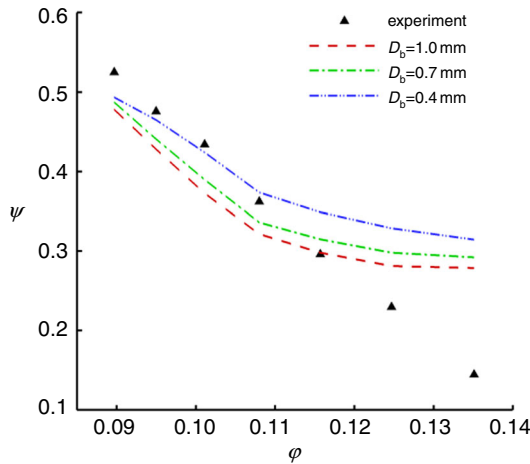


**Figure 2.** Head performance of the multiphase pump from the experiment and the numerical simulation with different bubble diameters

## 4. Results and discussions

### 4.1 Magnitude analysis of the interphase forces

For the conditions of  $IGVF \leq 30.2$  percent, i.e. the cases of Nos 1-5 listed in Table I, the area average of interphase forces are extracted along the flow passage, including the drag force, lift force, VMF and TDF. Figure 3 shows the magnitude ratio of non-drag forces to drag along the flow passage in three  $IGVF$  conditions, where  $z/L$  denotes the relative axial coordinate, and two vertical lines are used to represent the impeller inlet and outlet for convenience. From Figure 3, it can be seen that the TDF is negligible in the running of the multiphase rotodynamic pump relative to the drag, while the lift and VMF are comparable with it, and thus should not be ignored. As a whole, the magnitude ratios of lift/drag and VMF/drag will decrease along the streamwise direction, although some fluctuations occur in the vicinity of the impeller inlet and the domain inlet.

In the impeller region and the outlet extended region, the ratios of non-drag forces to drag are always substantially less than 1, regardless of the  $IGVF$  condition or the bubble size, which illustrates that the drag force is the dominant interphase force there. This can be explained through the contour distribution of gas void fraction shown in Figure 4. Due to the effect of centrifugal force (Yu *et al.*, 2012), the lighter gas phase tends to accumulate near the hub when it flows into the impeller region, and obvious separation of the two phases occurs in the outlet extended region. The inhomogeneous distribution makes the relative velocity of the two phases much larger than that in the inlet extended region, as shown in Figure 5. From Equation (5), we know that the drag will be much larger in these two regions and thus become the dominant interphase force.

In the inlet extended region, however, the lift and the VMF may be larger or smaller than the drag, depending on the  $IGVF$  condition and the axial position, as shown in Figure 3. According to Equations (9) and (10), the lift and the VMF may be smaller in regions with lower gas void fraction. Therefore, the magnitude ratios of lift/drag and VMF/drag are smaller when  $IGVF$  is 10.0 percent or 19.8 percent than that when  $IGVF$  is 30.2 percent. With the axial position nearer to the impeller, the ratios will also decrease due to the rotation effect of the impeller described above.

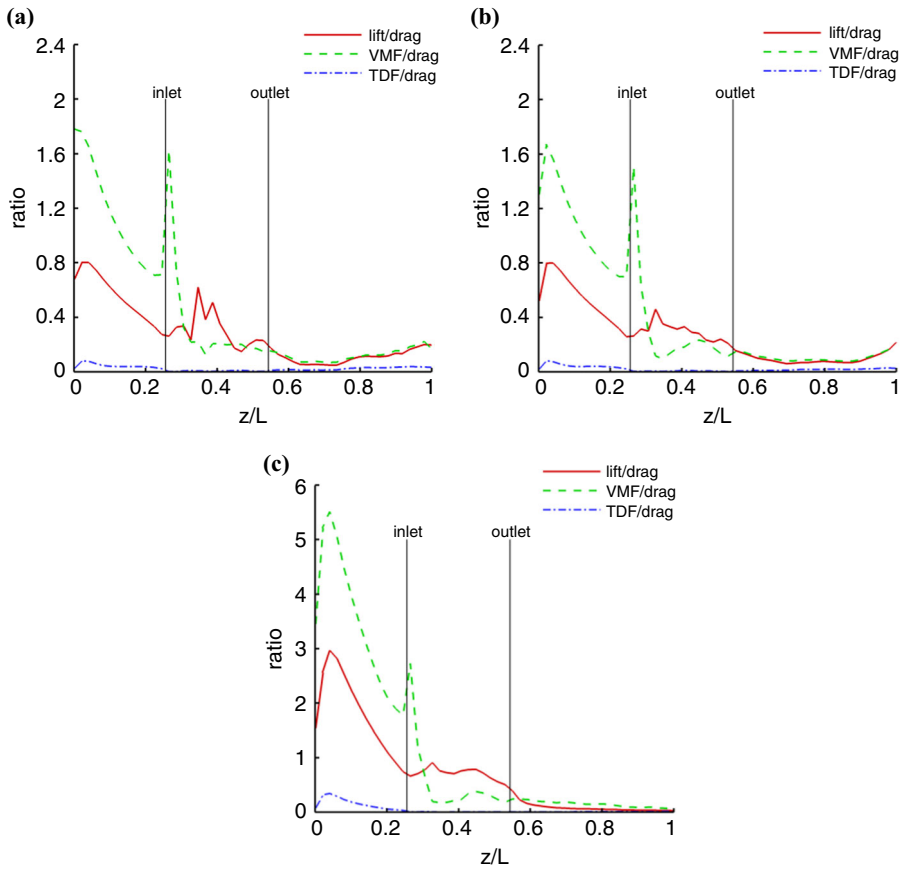


**Figure 3.**  
Magnitude ratios of non-drag forces to drag along the flow passage

**Notes:** (a) *IGVF*=10.0 percent,  $\phi = 0.090$  ( $D_b=0.4$  mm); (b) *IGVF*=19.8 percent,  $\phi = 0.101$  ( $D_b=0.4$  mm); (c) *IGVF*=30.2 percent,  $\phi = 0.116$  ( $D_b=1.0$  mm)

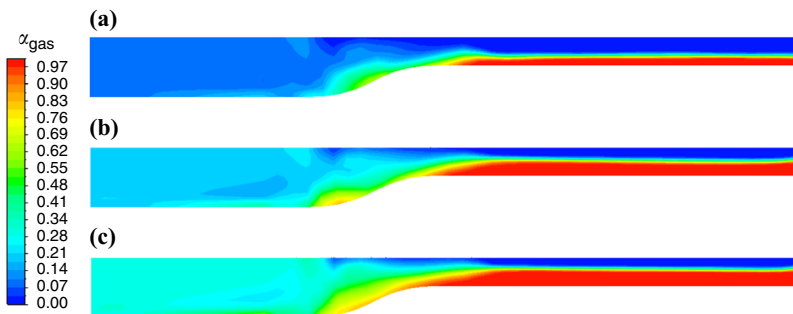


**Figure 4.**  
Contour distribution of gas void fraction

**Notes:** (a) *IGVF* = 10.0 percent,  $\phi = 0.090$  ( $D_b = 0.4$  mm); (b) *IGVF* = 19.8 percent,  $\phi = 0.101$  ( $D_b = 0.4$  mm); (c) *IGVF* = 30.2 percent,  $\phi = 0.116$  ( $D_b = 1.0$  mm)

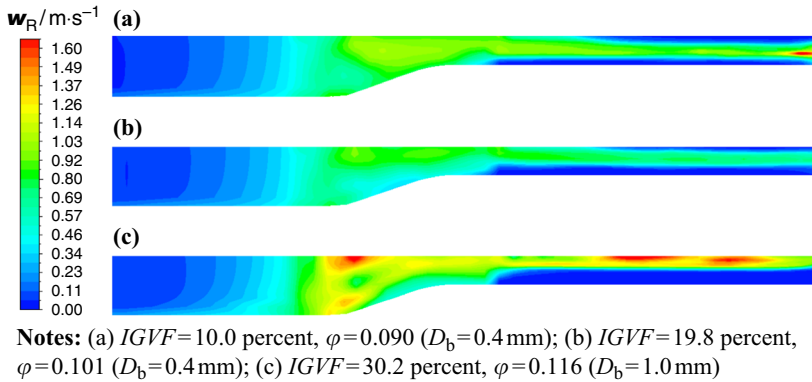


**Figure 5.**  
Contour distribution  
of the relative  
velocity between the  
two phases

Also, it can be found that the VMF is larger than the lift in the whole inlet extended region. Especially, in the region near the domain inlet, the value of VMF/drag is always greater than 1, which means the VMF there plays a dominant role among all the interphase forces including the drag. Therefore, in the simulation of gas-liquid two-phase flow in a multiphase rotodynamic pump, the VMF should be paid enough attention.

The characteristics of the two-phase distribution are closely connected with the magnitude information of the interphase forces. First, the onset of gas-liquid separation occurs in the region where all the ratios of non-drag forces to drag become less than 1, which is validated in Figures 3 and 4. To avoid this adverse phenomenon, we may improve the pump design from the point of restraining these force ratios. Second, the competition between the lift and the VMF may be a factor that leads to the radical variation of the gas void fraction in the impeller region, from which the systematical instability is originated. To get the fluctuation details of the gas void fraction and predict the separation process, transient simulation is needed, and this is our work in the next step.

#### 4.2 Sensitivity analysis of the bubble diameter

Figure 6 shows the magnitude variation of the interphase forces along the flow passage for different bubble sizes when  $IGVF$  equals 14.7 percent. In fact, the average bubble size in the flow passage is closely connected with the  $IGVF$  condition. As has been described in Section 3, in the condition of larger  $IGVF$ , larger bubble diameter should be set in the numerical model. Therefore, the goal in this part is to analyze the bubble size sensitivity in the numerical simulation. For the drag force, the influence of the bubble size is evident in the inlet extended region, i.e. larger bubble diameter is accompanied by smaller predicted magnitude of the drag force, while in the impeller region and the outlet extended region, the influence gets very slight. According to Equation (5), the factors that influence the drag include the drag coefficient  $C_D$ , the bubble diameter  $D_b$ , the gas void fraction  $\alpha_{\text{gas}}$  and the relative velocity  $w_R$ , where  $C_D$  is a function of the other three factors. If  $C_D$  is constant (although usually not; Crowe *et al.*, 2011), the drag force will be inversely proportional with  $D_b$ . Therefore, the effect of bubble size in the inlet extended region has played a dominant role.

For the lift force and VMF, in almost the whole flow passage, Figure 6 illustrates that the predicted values are larger if bigger bubble size is set. This may be because a

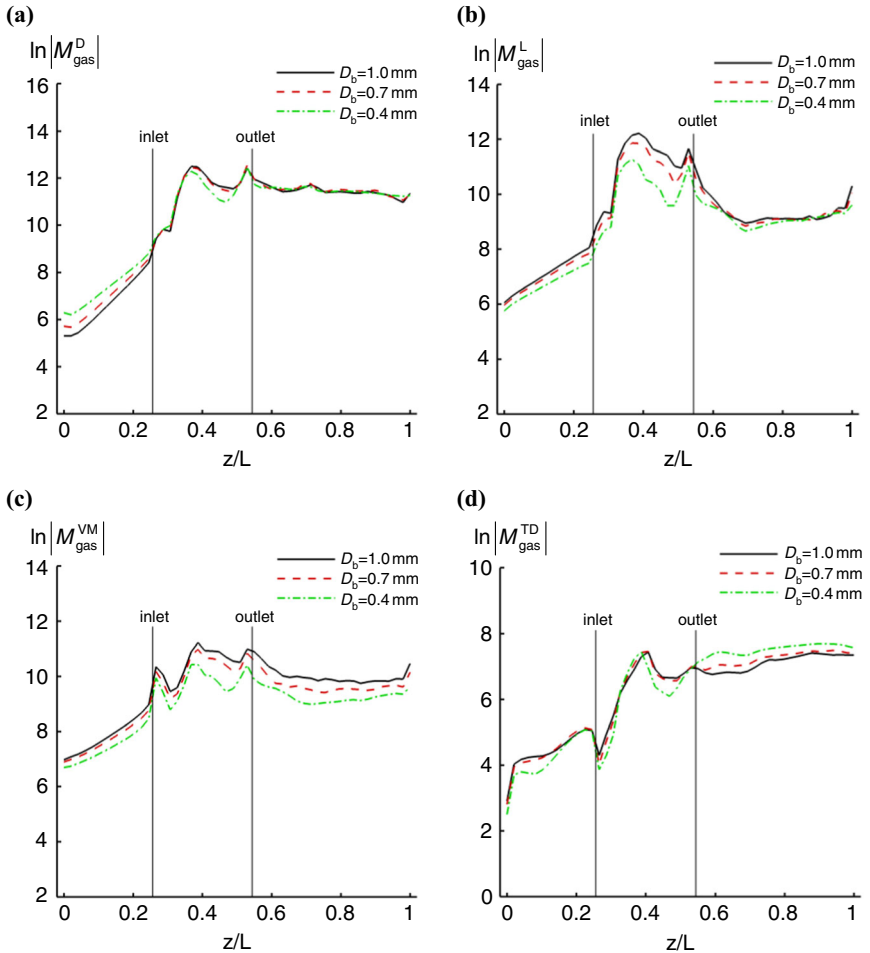


**Figure 6.** Magnitude variation of the interphase forces along the flow passage in different bubble sizes (*IGVF* = 14.7 percent, *n* = 1,500 rpm)

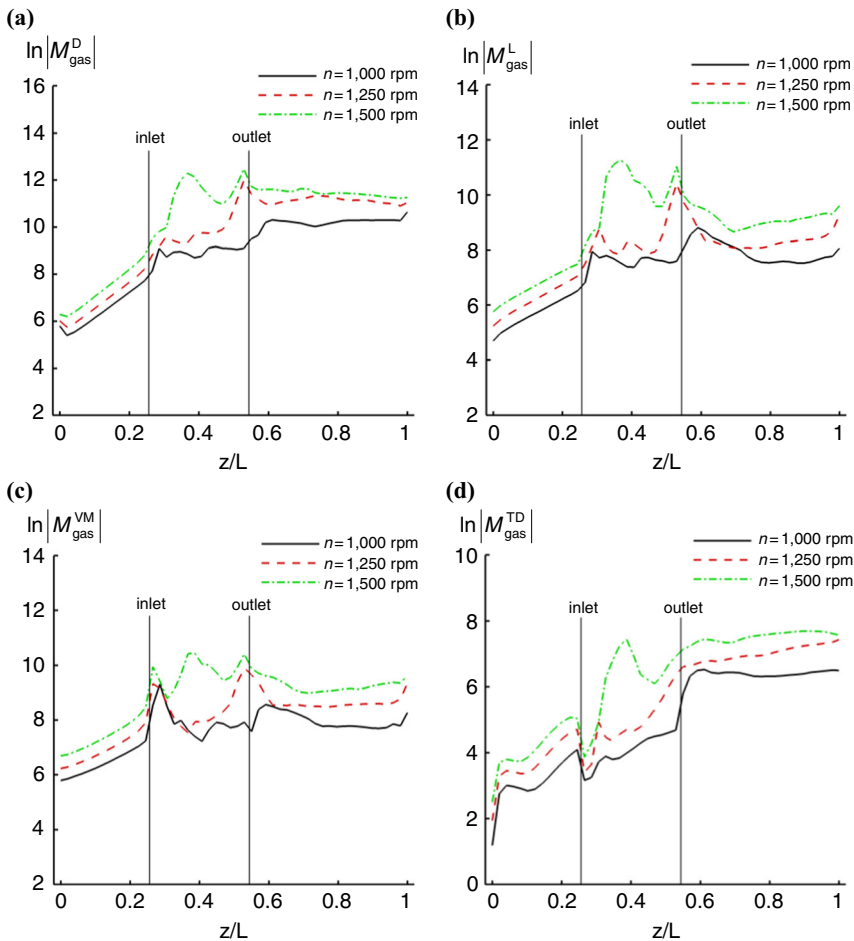
**Notes:** (a) Magnitude variation of drag force; (b) Magnitude variation of lift force; (c) Magnitude variation of virtual mass force; (d) Magnitude variation of turbulent dispersion force

bigger bubble size will lead to a higher level of gas void fraction in the flow field and thus, according to Equations (9) and (10), increase the values of the two forces. Finally, for the TDF, no distinct relation can be seen between the bubble size and the force magnitude.

Although the magnitudes of the interphase forces are different for different bubble sizes, the tendency of their variations along the streamwise direction seem not affected much by the bubble size condition. From Figure 6, it can be seen the magnitude of interphase forces is much larger in the impeller region and the outlet extended region than that in the inlet extended region, which shows that the rotation of the impeller can greatly increase the four interphase forces. Also, Figure 6 gives a further verification for the fact that the magnitudes of the drag, the lift and the VMF are comparable, whereas the TDF is much smaller.

4.3 Sensitivity analysis of the rotational speed

Similarly, the variation of the interphase forces along the streamwise direction in different rotational speeds is shown in Figure 7, where the bubble diameter is set 0.4 mm. As a whole, all the interphase forces will be raised by the increase of the rotational speed. This can be explained from the relation between the force scale and the velocity scale. According to the similarity theory (Potter and Wiggert, 2010), the force scale is proportional to the square of the velocity scale, which is closely associated with the rotational speed in rotating machinery. However, the actual variation of a force is also connected with many other factors, especially in multiphase flow. From the equations of the interphase forces in section 2.2, we know that the gas void fraction is an important factor. Therefore, in the impeller region, where pronounced change of gas



**Notes:** (a) Magnitude variation of drag force; (b) Magnitude variation of lift force; (c) Magnitude variation of virtual mass force; (d) Magnitude variation of turbulent dispersion force

**Figure 7.** Magnitude variation of the interphase forces along the flow passage for different rotational speeds ( $IGVF = 14.7$  percent,  $D_b = 0.4$  mm)

void fraction occurs (see Figure 4), the force variations with the rotational speed are more irregular than those in the two extended regions.

## 5. Conclusions

The interphase forces have important effects on the mixed transport process in a multiphase rotodynamic pump. In this paper, the gas-liquid two-phase flow is simulated by the two-fluid formulation, and the main interphase forces are analyzed in a series of *IGVFs*, bubble diameters and rotational speeds. The results can be summarized as follows:

- (1) For the simulation of bubbly flow in a multiphase rotodynamic pump, the bubble diameter is an important parameter and should be set according to *IGVF*. As the bubbles tend to coalesce in higher *IGVF* condition, larger bubble size should be adopted accordingly.
- (2) In the running of the multiphase rotodynamic pump, the magnitude of TDF is negligible relative to the drag, while the lift and VMF are comparable with it and the ratios of the two forces to drag will decrease along the streamwise direction.
- (3) In the impeller region and the outlet extended region, the drag force is the dominant interphase force due to the rotation effect; in the inlet extended region, however, the lift and the VMF may be larger or smaller than the drag, depending on the *IGVF* condition and the axial position.
- (4) The setting of bubble diameter will influence the predicted value of the drag, the lift and the VMF. Larger bubble diameter is accompanied by smaller predicted drag, but the effect is limited in the inlet extended region; for the lift and the VMF, the predicted values are larger if bigger bubble size is set.
- (5) The interphase forces will be raised with the increase of the rotational speed. In particular, due to the pronounced change of gas void fraction in the impeller region, this relationship becomes more irregular.

## References

- Bai, W., Deen, N.G. and Kuipers, J.A.M. (2011), "Numerical analysis of the effect of gas sparging on bubble column hydrodynamics", *Ind. Eng. Chem. Res.*, Vol. 50 No. 8, pp. 4320-4328.
- Benhmide, A., Chaouachi, B., Bourouis, M. and Gabsi, S. (2011), "Numerical prediction of flow patterns in bubble pumps", *J. Fluids Eng.*, Vol. 133 No. 3, 031302.
- Bertodano, M.L., Lahey, R.T. and Jones, O.C. (1994), "Turbulent bubbly two-phase flow data in a triangular duct", *Nucl. Eng. Des.*, Vol. 146 Nos 1/3, pp. 43-52.
- Cao, S.L., Peng, G.Y. and Yu, Z.Y. (2005), "Hydrodynamic design of rotodynamic pump impeller for multiphase pumping by combined approach of inverse design and CFD analysis", *J. Fluids Eng.*, Vol. 127 No. 2, pp. 330-338.
- Chen, P., Dudukovic, M.P. and Sanyal, J. (2005), "Three-dimensional simulation of bubble column flows with bubble coalescence and breakup", *AIChE J.*, Vol. 51 No. 3, pp. 696-712.
- Crowe, C.T., Schwarzkopf, J.D., Sommerfeld, M. and Tsuji, Y. (2011), *Multiphase Flows with Droplets and Particles*, 2nd ed., CRC Press, Boca Raton, FL.
- Deen, N. (2001), "An experimental and computational study of fluid dynamics in gas-liquid chemical reactors", PhD thesis, Aalborg University, Esbjerg, August.

- Deen, N.G., Solberg, T. and Hjertager, B.H. (2001), "Large eddy simulation of the gas-liquid flow in a square cross-sectioned bubble column", *Chem. Eng. Sci.*, Vol. 56 Nos 21/22, pp. 6341-6349.
- Dhotre, M.T., Deen, N.G., Niceno, B., Khan, Z. and Joshi, J.B. (2013), "Large eddy simulation for dispersed bubbly flows: a review", *Int. J. Chem. Eng.*, Vol. 2013 No. 2013, Article ID 343276, pp. 1-22.
- Diaz, M.E., Iranzo, A., Cuadra, D., Barbero, R., Montes, F.J. and Galan, M.A. (2008), "Numerical simulation of the gas-liquid flow in a laboratory scale bubble column: influence of bubble size distribution and non-drag forces", *Chem. Eng. J.*, Vol. 139 No. 2, pp. 363-379.
- Falcimaigne, J., Brac, J., Charron, Y., Pagnier, P. and Vilagines, R. (2002), "Multiphase pumping: achievements and perspectives", *Oil Gas Sci. Technol. – Rev. IFP*, Vol. 57 No. 1, pp. 99-107.
- Gupta, A. and Roy, S. (2013), "Euler-Euler simulation of bubbly flow in a rectangular bubble column: experimental validation with radioactive particle tracking", *Chem. Eng. J.*, Vol. 225, pp. 818-836.
- Hajem, M., Morel, R., Champagne, J., Vilagines, R. and Pagnier, P. (2001), "The study of the flow in an helico-axial pump using laser Doppler velocimetry", *La Houille Blanche, Revue Internationale De L'Eau*, Nos 3/4, pp. 34-39.
- Johnson, R.W. (1998), *The Handbook of Fluid Dynamics*, CRC Press, Boca Raton, FL.
- Kendoush, A.A. (2005), "The virtual mass of a rotating sphere in fluids", *J. Appl. Mech.*, Vol. 72 No. 5, pp. 801-802.
- Krepper, E., Beyer, M., Frank, T., Lucasa, D. and Prasser, H-M. (2009), "CFD modelling of polydispersed bubbly two-phase flow around an obstacle", *Nucl. Eng. Des.*, Vol. 239 No. 11, pp. 2372-2381.
- Laborde-Boutet, C., Larachi, F., Dromard, N., Delsart, O. and Schweich, D. (2009), "CFD simulation of bubble column flows: investigations on turbulence models in RANS approach", *Chem. Eng. Sci.*, Vol. 64 No. 21, pp. 4399-4413.
- Lahey, R.T., Bertodano, M.L. and Jones, O.C. (1993), "Phase distribution in complex geometry conduits", *Nucl. Eng. Des.*, Vol. 141 Nos 1/2, pp. 177-201.
- Levy, A., Koyfman, A. and Jelinek, M. (2006), "Flow boiling of organic binary mixtures", *Int. J. Multiphase Flow*, Vol. 32 Nos 10/11, pp. 1300-1310.
- Liu, D.Y. (1993), *Fluid Dynamics of Two-Phase Systems*, Higher Education Press, Beijing.
- Menter, F.R. (1994), "Two-equation eddy-viscosity turbulence models for engineering applications", *AIAA J.*, Vol. 32 No. 8, pp. 1598-1605.
- Mohajerani, M., Mehrvar, M. and Ein-Mozaffari, F. (2012), "CFD analysis of two-phase turbulent flow in internal airlift reactors", *Can. J. Chem. Eng.*, Vol. 90 No. 6, pp. 1612-1631.
- Potter, M.C. and Wiggert, D.C. (2010), *Ramadan, B.H. Mechanics of Fluids*, 4th ed., Cengage Learning, Stamford, CT.
- Pourtousi, M., Sahu, J.N. and Ganesan, P. (2014), "Effect of interfacial forces and turbulence models on predicting flow pattern inside the bubble column", *Chem. Eng. Process.*, Vol. 75, pp. 38-47.
- Seixlack, A.L. and Barbazelli, M.R. (2009), "Numerical analysis of refrigerant flow along non-adiabatic capillary tubes using a two-fluid model", *Appl. Therm. Eng.*, Vol. 29 Nos 2/3, pp. 523-531.
- Tabib, M.V. and Schwarz, P. (2011), "Quantifying sub-grid scale (SGS) turbulent dispersion force and its effect using one-equation SGS large eddy simulation (LES) model in a gas-liquid and a liquid-liquid system", *Chem. Eng. Sci.*, Vol. 66 No. 14, pp. 3071-3086.
- Tabib, M.V., Roy, S.A. and Joshi, J.B. (2008), "CFD simulation of bubble column – an analysis of interphase forces and turbulence models", *Chem. Eng. J.*, Vol. 139 No. 3, pp. 589-614.

- Tan, L., Cao, S.L., Wang, Y.M. and Zhu, B.S. (2012), "Influence of axial distance on pre-whirl regulation by the inlet guide vanes for a centrifugal pump", *Sci. China Technol. Sc.*, Vol. 55 No. 4, pp. 1037-1043.
- Tan, L., Zhu, B.S., Cao, S.L., Hao, B. and Wang, Y.M. (2014), "Influence of blade wrap angle on centrifugal pump performance by numerical and experimental study", *Chin. J. Mech. Eng-En.*, Vol. 27 No. 1, pp. 171-177.
- Troshko, A.A. and Hassan, Y.A. (2001), "A two-equation turbulence model of turbulent bubbly flows", *Int. J. Multiphase Flow*, Vol. 27 No. 11, pp. 1965-2000.
- Yan, K. and Che, D.F. (2010), "A coupled model for simulation of the gas-liquid two-phase flow with complex flow patterns", *Int. J. Multiphase Flow*, Vol. 36 No. 4, pp. 333-348.
- Yang, L. and Zhang, C.L. (2005), "Two-fluid model of refrigerant two-phase flow through short tube orifice", *Int. J. Refrig.*, Vol. 28 No. 3, pp. 419-427.
- Yu, Z.Y. (2005), "Numerical simulation of gas-liquid two-phase flow and experimental study on a multiphase rotodynamic pump", PhD thesis, Tsinghua University, Beijing, April.
- Yu, Z.Y., Zhang, Q.Z., Huang, R. and Cao, S.L. (2012), "Numerical analysis of gas-liquid mixed transport process in a multiphase rotodynamic pump", *26th IAHR Symposium on Hydraulic Machinery and Systems, Beijing, August 19-23*, Vol. 15 No. 3.
- Zhang, D., Deen, N.G. and Kuipers, J.A.M. (2006), "Numerical simulation of the dynamic flow behavior in a bubble column: a study of closures for turbulence and interface forces", *Chem. Eng. Sci.*, Vol. 61 No. 23, pp. 7593-7608.

**Corresponding author**

Dr Zhiyi Yu can be contacted at: [yuzhiyi@bit.edu.cn](mailto:yuzhiyi@bit.edu.cn)